Near infrared performance of a pile-of-plates polariser based on poly-crystalline Zinc Selenide

Qianliang Li[a*,b], Walter Perrie[b*], Tong Zhou[c,b], Zheng Fang[b], Stuart Edwardson[b], Geoff Dearden[b]

[a]Laser Group, School of Mechanical Engineering, Hubei University of Technology, Wuhan, 430068, China
[b]Laser Engineering Group, School of Engineering, Brownlow Street, University of Liverpool, Liverpool, L69 3GQ, United Kingdom
[c]College of Science, Jiangsu University of Science and Technology, Zhenjiang, 212100, China

Abstract : Zinc Selenide (ZnSe) has wide transparency from 0.6 μm – 18 μm making it a desirable substrate for infrared (IR) optical applications. We present experimental results on the NIR transmission of a pile-of-plates polariser at 780 nm and 1.06 μm based on polycrystalline ZnSe plates tilted at Brewster's angle. Due to the high refractive index of ZnSe, n ~ 2.5, the degree of polarisation (DOP, V) at λ = 780 nm and 1.06 μm reached V = 0.98 and 0.97 respectively with 4 plates and an extinction ratio E < 10^{-2} at 780 nm. The calculated DOP for 1 – 4 plates agree well with theory when allowance is made for internal surface reflections, as in the Airy expressions. While the DOP achieved with 4, 1 mm thick plates is relatively high, the absolute transmission for the P component (T_P = 0.83, 0.84 respectively) is much lower than expected, based on the NIR extinction coefficients k < 10^{-6} (780 nm) and k ~10^{-7} (1.06 μm), inferring T_P > 0.96. The source of this absolute loss has been considered, including residual surface scatter, diffuse scatter from grain boundaries in the polycrystalline micro-structure and the likely effect of residual birefringence. This loss, we believe is primarily due to residual surface scatter in thin crystal lattice damage layers created during the polishing process and observed when using a hand-held near infrared (NIR) camera. This scatter is polarisation dependent as expected but much higher than scatter theory predicts, consistent with crystalline surface damage. A 6-plate assembly demonstrated an extinction ratio of 1/600 and transmission T_p ~ 0.72 at 1.06 μm. The very low absorption and dispersion in ZnSe, particularly at longer wavelengths infer that this polariser would work well in the important MIR region.

Keywords: polycrystalline ZnSe, broadband polariser, extinction coefficient, scattering.

1 Introduction

Polarisation of radiation, its analysis and manipulation remain at the forefront of scientific advances in disparate fields. In Astrophysics for example, the polarisation of the cosmic microwave background carries information on the distribution of matter in the early universe [1] while in Atomic physics, the threshold polarisation of atomic line emissions allow sensitive tests of the theory of electron-atom collisions [2]. In addition, ellipsometry allows determination of the optical constants (n,k) of materials (metals, semi-conductors) [3] while the creation of complex polarisation fields carrying Optical Angular Momentum (OAM) is relevant to increasing resolution in microscopy and communications bandwidths [4]. Engineered metamaterial surfaces with planar nano-structures can allow arbitrary manipulation of polarisation profiles in reflection and transmission [5]. In the optical region, polarising elements include dichroic absorbers made from polymer sheets, polarising dielectric films and birefringent materials such as calcite used in Glan-Taylor and Glan-Thomson polarisers [6]. Polymer sheets are limited mainly to visible wavelengths with good extinction ratios whereas multi-layer dielectric films have narrow bandwidths hence generally used at laser wavelengths. Polarising prisms made of Calcite offer very high extinction ratios < 10^{-4}, high transmission and often used in laser applications, however, their wavelength range is limited over 0.3 μm - 2.3 μm [7] due to material absorption at these limits. In the Mid-infrared (MIR) and Far-infrared (FIR) spectral regions, wire grid polarisers created photolithographically on transparent substrates such as ZnSe have a useful range up to 14μm. On the other hand, free standing wires can cover wavelengths λ > 100 μm [6]. One drawback here, however is the delicate nature of these devices.

When unpolarised light passes through a series of tilted transparent dielectric plates, the consequence of sequential Fresnel reflections, where S polarised reflection coefficient $R_s > R_p$ leads to an increasing degree of polarisation of the transmitted light with plate number N. By tilting plates to the Brewster angle $\theta_B = \tan^{-1}n$ where n is the plate refractive index, this yields a pile-of-plates (POP) polariser with high transmission for the P polarised component since $R_p(\theta_B) \sim 0$. In an optical region of low dispersion, where refractive index varies slowly, this type of polariser has a wide operating bandwidth. Also, the higher the material refractive index, the more effective is the DOP of a single plate hence reducing the number of plates required to achieve a good extinction ratio.

The literature on the transmission of light through a series of transparent or absorbing parallel sided glass plates has a remarkable history going back to Fresnel [8] and calculated, independently by, for example, Stokes in Cambridge [9]. A concise review of the history of reflection of light from a pile of plates (POP) was given by Tuckerman [10] who realised that occasionally, incorrect transmission formulae were quoted due to omission of the effect of multiple reflections taking place between the parallel plate surfaces. Tuckerman's analysis for transparent glass plates predicted reflection/transmission coefficients in agreement with Fresnel and Stokes.

The polarisation performance of a series of Selenium films (n = 2.45) in the Infrared were investigated by Conn and Eaton [11] and Greenler et al [12]. Conn and Eaton showed that interference effects were neglible as phase differences could be regarded as randomly distributed. They also demonstrated that the DOP measured from a series of Zapon Laquer films in the visible region well exceeded the predicted performance, showing convincingly that this effect was due to the size of the limiting aperture which restricts the number of multiple reflections (S polarised) between the films, increasing the DOP.

Weinberger presented a detailed theoretical analysis of expected POP polariser performance of transparent glass plates as a function of angle of incidence (AOI), refractive index n (1.5 - 2.0) and plate numbers N (1, 2, 5, 10) for both single/multiply reflected rays [13]. The analysis clearly shows the detrimental effect on DOP when including multiple reflections between plates by increasing aperture. Hence, even with 10 AgCl plates with a relatively high RI, n = 2.01, the expected DOP = 0.850 at Brewster's angle ($\theta_B = 63.5°$). The maximum DOP with multiple reflections included appears approximately 10° above Brewster's angle.

UV transparent POP polarisers based on synthetic fused silica plates (N = 12) were used in the polarisation analysis of the 2-photon UV/visible continuum emission from the $2S_{1/2}$ metastable state in atomic deuterium [14]. This continuum radiation is centred near 243nm and the measured transmittances with linearly polarised light at λ = 254 nm (Hg line) yielded $T_p = 0.94$ and $T_s = 0.03$ respectively, hence achieving a DOP = 0.938. In this case, a high absolute transmission for the P component was essential for a critical test of Bell's inequality [15] with QM entangled photon pairs. Aspect also achieved a similar DOP with 10 glass plate POP polarisers in tests of photon entanglement [16]. During Organic Light Emitting Diode (OLED) display manufacture, a UV polariser based on fused quartz plates for photo-alignment layer exposure is regarded as superior to a wire grid polariser in terms of cost and scalability [17]. A fused silica POP polariser used during electron impact excitation of the Zn 4^1P_1 atomic state at λ = 213.8nm allowed Stokes parameter determination during e-photon coincidence measurements [18]. A low birefringence optical polarisation magnifier based on 6 wedged fused silica plates (Herasil) achieved a magnification factor k ~3 [19].

Low cost, very broad bandwidth POP polarisers based on three plate polished n-type Silicon wafers (0.35 × 15 × 50 mm) were developed for use in a FTIR spectrometer and demonstrated impressive performance over a remarkable wavelength range [20]. With polarisers crossed, transmission T < 0.5% from 1.4 -10 μm while between 20 μm and 100 μm, T < 2.5%. Semi-conductor grade Silicon therefore produces a very useful broad bandwidth POP polariser. A reflective type POP polariser, where the S component was successively reflected from 4 Ge plates at Brewster's angle (chevron geometry) achieved very high extinction ratios ($< 10^{-5}$) over the wavelength range $0.633 \leq \lambda \leq 10.6\mu m$ with transmission $T_s \sim 0.4$-0.5 [21]. Recently, a highly effective POP polariser based on 4 Si plates achieved extinction ratio $< 10^{-4}$ over the wavelength range 1.6μm – 6.5μm while demonstrating the separation of signal and idler beams from a broadband MIR optical parametric source [22].

Zinc Selenide is an important compound semi-conductor material used in a wide range of applications such as blue-green and white light emitting laser diodes, tunable mid-IR lasers for remote sensing and photovoltaic applications [23]. The material has a wide optical bandwidth, transparent from the visible to the MIR, λ = 0.6 μm - 16 μm hence an excellent MIR window material. Its refractive index is high, varying from n = 2.6 to 2.4 over this range with very low absorption coefficient quoted as $\alpha \sim 5.10^{-4}\,cm^{-1}$ at 1.3 μm [24]. Its high transparency and refractive index therefore suggest that ZnSe should be an ideal substrate for a wide band POP polariser.

A review of polarisers for the IR region was presented by Bennet in 1995 [6]. Infrared POP polarisers included Se films, AgCl, Ge, ZnS, KRS-5(Thallium Bromo-iodide) and polyethylene. A single reference to a ZnSe POP polariser (6 plate) used in an IR ellipsometer was acquired commercially [25]. No geometrical details other than plate number

are given. Extinction ratio over $\Delta\lambda$ = 3.4 - 4.0 μm was quoted as 1/800 with angular acceptance of 2° and beam deviation $\Delta\theta$ < 0.3 mR, so achieving an excellent performance.

The polycrystalline material used here is fabricated by CVD which results in very pure material with a cubic structure. Transmission measurements were carried out with linearly polarised laser sources, 780 nm (10 ns) and 1064 nm (10ps) to confirm POP performance.

2 Experimental

Two laser sources were utilised for experimental tests. Firstly, a linearly polarised laser beam (Clarke-MXR, CPA-2010, 780 nm /10 ns/1 kHz) was produced by an unseeded re-generative amplifier system with output Gaussian beam diameter φ = 5mm $1/e^2$. The polariser performance was checked experimentally by measuring transmitted power while rotating a half-wave plate HWP (zero order, Newport). Incident and transmitted average powers (P <100 mW) were measured with a 3 W Coherent PM while for more sensitive tests, a pyro-electric detector was employed, measuring every pulse at 1 kHz (3 Sigma, Molectron J5-09). The linearly polarised laser source at 1.06μm was a seeded Regenerative amplifier system producing 10ps pulses at 5kHz repetition rate (High Q model IC-355-800).

2.1 Polariser design

Fig.1 shows the geometry used for the 4 plate ZnSe POP polariser (not to scale) with plates set at Brewster's angle. The plates are stacked oppositely to compensate off axis deviations so that the transmitted beam stays on axis. As the incident unpolarised beam suffers both surface and internal reflections, the DOP improves with transmission since the P component has $R_p = 0$ while the S component is attenuated through reflections at each interface.

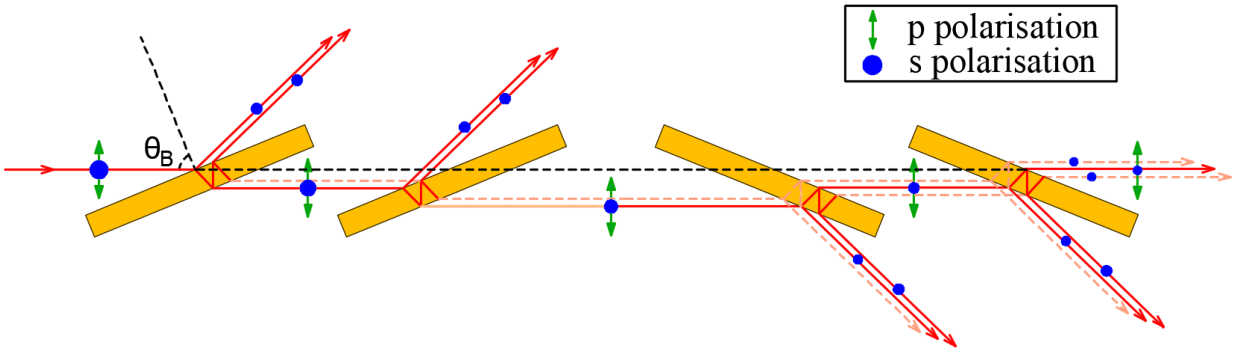

Fig. 1. The transmission and reflection of an incident unpolarised beam in a 4 plate POP polariser showing the attenuation of the unwanted S component by reflection near Brewster's angle. The DOP increases after every plate through surface reflections. Shown also is an internally reflected S component (dashed lines) which, after transmission, result in low intensity off axis rays at the POP output. These S polarised rays spoil the effective DOP. No reflections between plates occur due to the large Brewster angle and plate separation. Interference within plates is regarded as neglible as phase differences between interfering components are randomly distributed [11].

The POP polariser device (28 × 50 × 1.0 mm) was constructed using four plates of polycrystalline ZnSe, as shown in the photo, Fig. 2. The polished plates (Ra ~ 8 nm) were mounted in Teflon sleeves with slots milled at 68.4° to the horizontal axis. Plate separation (in each pair) along the optic axis was 26 mm (10 mm between parallel faces). Teflon inserts were attached to the inside of a rectangular Aluminium frame with input and output apertures of 10 mm diameter. Copper plates (with roughened matt surfaces) were mounted top and bottom to absorb the reflected S-polarised components – useful, for example in potential low-power laser applications at the CO_2 laser wavelength, 10.6 μm. The end sections were mounted in rotation stages (Thorlabs RSP1), so that the whole assembly could be rotated easily.

Fig. 2. Photo of the 4 plate POP polariser device using rectangular polycrystalline ZnSe plates, 1.0 mm thick with separation 26 mm along the optic axis, avoiding multiple reflections between plates. The assembly was supported on rotational stages either end.

2.2 Expected performance

Expected DOP from the POP polariser can be estimated from the Fresnel reflection coefficients [26] for the P and S components of an incident unpolarised beam. To achieve a reasonable DOP, we need to reduce the transmitted S component intensity to < 1% Assuming the incident wavelength λ = 780nm, the refractive index n = 2.53 [24], and Brewster's angle $\theta_B = \tan^{-1}(2.53) = 68.43°$. Consider a single transparent ZnSe plate tilted at Brewster's angle. The reflectivity of S polarised light from the first air/ZnSe interface is given by the Fresnel coefficient [26],

$$r_s = [\frac{\sin(\theta_i - \theta_r)}{\sin(\theta_i + \theta_r)}]^2 \quad (1)$$

where θ_i is the angle of incidence and θ_r is the angle of refraction. At λ = 780nm, $\theta_i = \theta_B = 68.43°$ hence using Snell's law, $\sin\theta_r = 0.3676$ and $\theta_r = 21.57°$ yielding $r_s = 0.532$ and $t_s = (1- r_s) = 0.468$ at a single interface. Ignoring internal multiple reflections between faces, a single plate transmission would yield $T = t_s^2 = (0.468)^2 = 0.219$ and for 4 plates, $T_s^4 = (0.219)^4 = 0.0023$ with a DOP V = (1-0.0023) / (1+0.0023) = 0.995, well overestimating the actual DOP.

Allowing for multiple internal reflections within the plates, assuming interference is neglible, the coefficients for the reflected and transmitted intensities from a single plate are then given by the Airy expressions [11],

$$R_s = \frac{(n^2-1)^2}{(n^4+1)} \quad (2)$$

$$T_s = 1 - R_s = \frac{2n^2}{n^4+1} \quad (3)$$

Setting n = 2.53 at λ = 780 nm, we immediately obtain $R_S = 0.695$ and $T_S = 0.305$ for a single plate. This was confirmed by calculating the individual transmitted components through one plate and summing these (based on Fresnel reflection at a single interface, ($r_s = 0.532$, $t_s = 0.468$) yielding $T_S = t_s^2 + t_s^2r_s^2 + t_s^2r_s^4 + t_s^2r_s^6 + t_s^2r_s^8 + \ldots.$ = 0.219 + 0.062 + 0.018 + 0.005+ 0.001+….= 0.305 with 5 components, in agreement with the Airy expression (3) above. Hence for 4 plates we expect the S component to be attenuated to $(T_S)^4 = (0.305)^4 = 8.65 \times 10^{-3}$ (<1%) with expected DOP V = (1- 0.00865) / (1+ 0.00865) = 0.983 and extinction ratio $E = T_s / T_p = 0.009$.

The calculated changes of the DOP with an incident unpolarised beam (V = 0) passing through ZnSe plates (N =1 - 4) are listed in Table 1 where DOP_{th} $V = [1- (T_S)^N / (1+ (T_S)^N)]$. As expected, V increases significantly with plate number and a good performance polariser with V = 0.983 can be achieved with only 4 plates of ZnSe. This is in complete contrast to a pile-of-plates polariser made from synthetic fused silica (n = 1.5) where 12 plates were required to achieve a DOP V = 0.95 [14]. Also shown is the effect of adding 2 more plates which brings V = 0.998 and extinction ratio < 10^{-3}, although at the cost of increasing the polariser length.

Table 1. Calculated DOP at λ = 780 nm with plate number N. A 4 plate ZnSe POP should therefore achieve V > 0.98 by reducing the S component to < 1%.

N (number of plates)	$(T_s)^N$	DOP_{th}
1	0.305	0.533
2	0.093	0.830
3	0.028	0.945
4	0.0087	0.983
6	0.00081	0.998

3 Results and discussion

3.1 Transmission at λ = 780 nm

The transmission at 780 nm of 1 - 4 ZnSe plates mounted in the POP polariser when rotating a HWP plate is shown in Fig.3. As expected, the minima occur at 45°, 135° and 225°. The solid lines are best fits to the data based on the expected transmission function, $T = A\cos^2(2\theta_{HWP}) + B$, so that A and B, extracted from the fits yield the DOP, V = (A-B) / (A+B). Based on the fits, we find A = 0.75, B = 0.22 (N=1), A= 0.85, B= 0.08 (N=2), A = 0.85, B = 0.02 (N=3) and A = 0.82, B = 0.008 for N = 4. Hence, the measured DOP, V = 0.54, 0.83, 0.94 and 0.98 for N=1- 4 respectively with extinction ratio for 4 plates $E < 10^{-2}$. The measured transmission coefficients for P and S components are summarised in Table 2 with a comparison of experimental and theoretically expected DOP with excellent agreement.

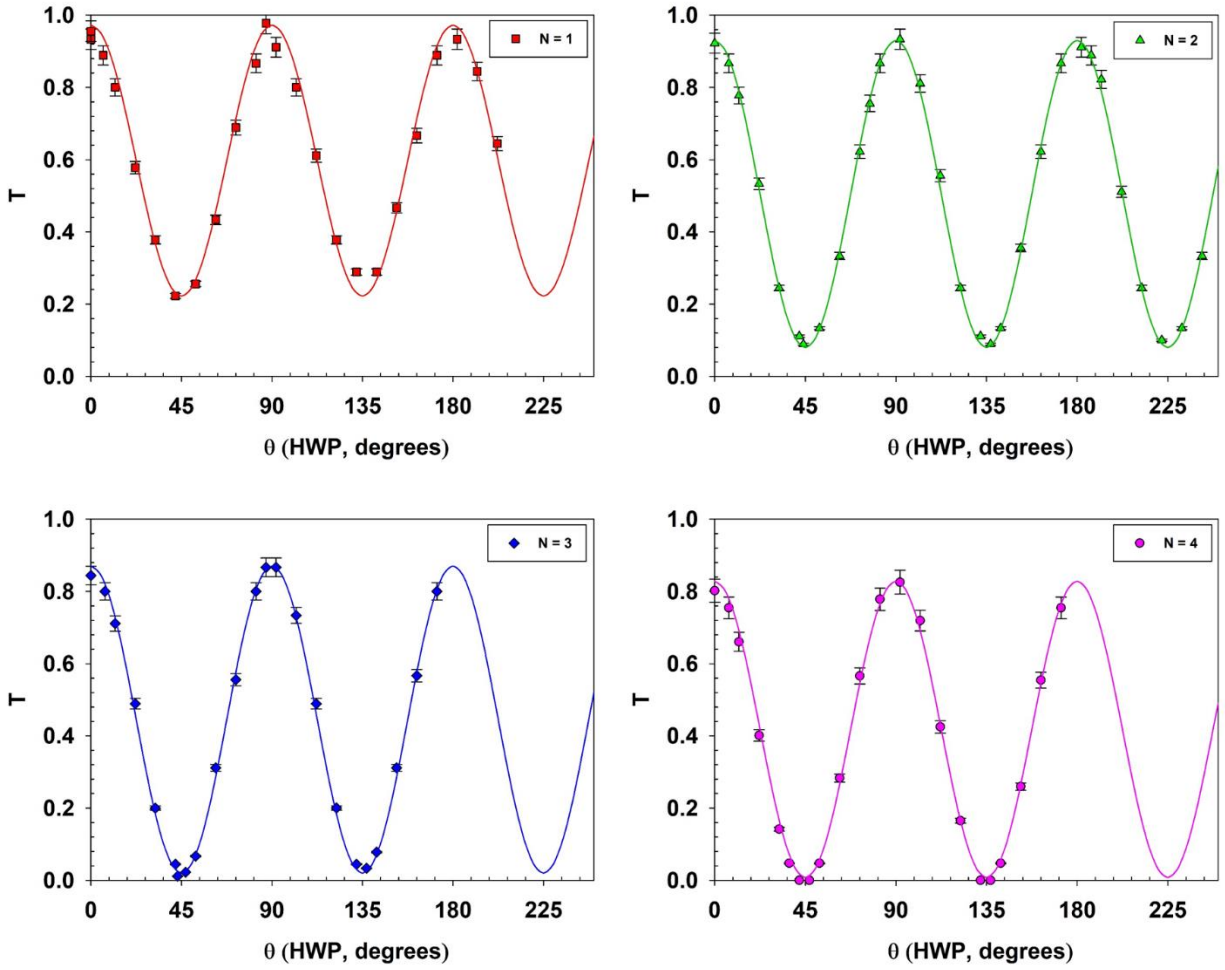

Fig. 3. Measured transmission at λ = 780 nm for 1 - 4 ZnSe plates mounted in the POP polariser when rotating a HWP plate.

Table 2. Measured transmission for P and S components at 780 nm and DOP_{exp} compared with DOP_{th} expected from the Airy expressions. Errors quoted are 1σ.

N (number of plates)	T_P	T_s	DOP_{exp}	DOP_{th}
1	0.97 ± 0.03	0.287 ± 0.004	0.54 ± 0.02	0.533
2	0.93 ± 0.03	0.082 ± 0.001	0.83 ± 0.03	0.830
3	0.87 ± 0.03	0.026 ± 0.001	0.94 ± 0.03	0.945
4	0.83 ± 0.03	0.008 ± 0.001	0.98 ± 0.04	0.983

The drop in absolute transmission with plate number (increasing optical thickness) was surprising, based on the measured optical constants of ZnSe in the NIR [27]. At 780nm, the measured value of extinction coefficient in ZnSe, $k_{780} = 0.38\times10^{-6}$ hence the absorption coefficient $\alpha = (4\pi k)/\lambda = 0.061$ cm^{-1}. The optical path length through a t = 1.0 mm thick plate is $L = t/\cos\theta_r$ where $\theta_r = 21.57°$, hence $L_1 = 1.075$ mm/plate and optical path length of 4 plates L = 4.30 mm = 0.43 cm. The expected transmission for the P component at Brewster's angle should then be $T_p = e^{-\alpha L} = 0.97$, a

3% loss. Even at Brewster's angle, low intensity specularly reflected beams were observed using a hand held NIR camera and measured carefully using the pyro-electric detector, yielding 0.25%/plate – hence a 1% additional loss due to surface imperfections or deviation of the plates from the Brewster angle. Put together, the absolute transmission for 4 plates should therefore reach $T_P = 0.96$, well above the observed value of 0.83.

3.2 Transmission at λ = 1.06 μm

The observed transmission of the POP polariser at the laser wavelength, 1.06 μm (10 ps / 5 kHz) was measured using a sensitive Si detector (Coherent LM2/Fieldmaster), Fig.4. The incident Gaussian beam was apertured to approximately ~5 mm diameter. Fig.4(a) shows the observed transmission when rotating the POP polariser while Fig.4(b) shows the transmission when rotating a zero order HWP plate. The fits to the data show $T = A\cos^2(2\theta_{HWP}) + B$ and $T = A\cos^2(\theta_{POP}) + B$ (A = 0.84, B = 0.01) respectively. Again, we have a good performance with DOP V = 0.97 and extinction ratio E = 0.012. The absolute transmission $T_P = 0.85$, again lower than expected. At 1.06 μm, where $k \sim 10^{-7}$ [27], $\alpha_{1064} = 0.017 cm^{-1}$ hence expect $T_P = 0.993$ with an absorption loss of only 0.7%. Allowing for a 1% total specular reflection loss (as with 780 nm), we would expect $T_P = 0.983$, much higher than observed.

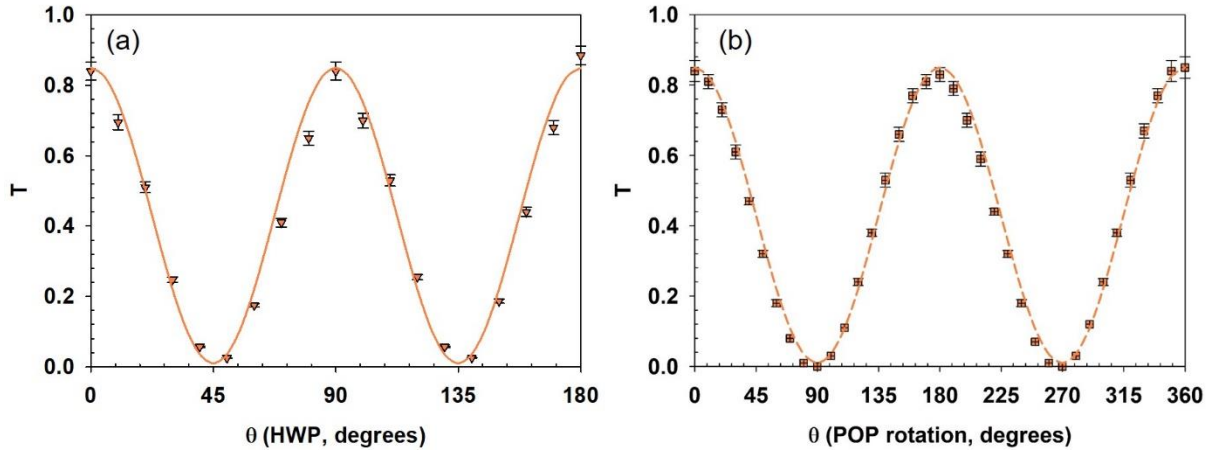

Fig. 4. Observed transmission of the 4 plate ZnSe POP polariser with a linearly polarised laser beam at λ = 1.064 μm (10 ps / 5 kHz). (a) when rotating HWP; (b), when rotating POP polariser. The incident beam diameter was φ = 5 mm and measured DOP V = 0.97 ± 0.02 with absolute transmission for the P component $T_P = 0.84 \pm 0.01$. The best fits to the data are $T = 0.83\cos^2(2\theta_{HWP})+0.01$ and $0.83\cos^2(\theta_{POP})+0.01$ with good agreement.

When altering the number of plates from N =1-4, and rotating HWP, we obtained $T_P = 0.95, 0.92, 0.89, 0.84$ respectively while $T_s = 0.306, 0.106, 0.036, 0.012$ respectively. T_p decreases nearly linearly with N while T_s decreases exponentially.

Using a camera (Spiricon SP620U), the beam position and intensity change at 1.064 μm with POP rotation angle is shown in Fig. 5. These images show one of the drawbacks of transmissive POP polariser characteristics which can result in angular offset when rotating the plates. This shift may be caused by variation of the slight residual wedge angles and contribution from errors in mechanical mounting of the plates. The angular offset here is approximately Δφ ~ 5 mR but could be substantially eliminated by introducing small, well defined plate wedges while also fanning the plate angles [28].

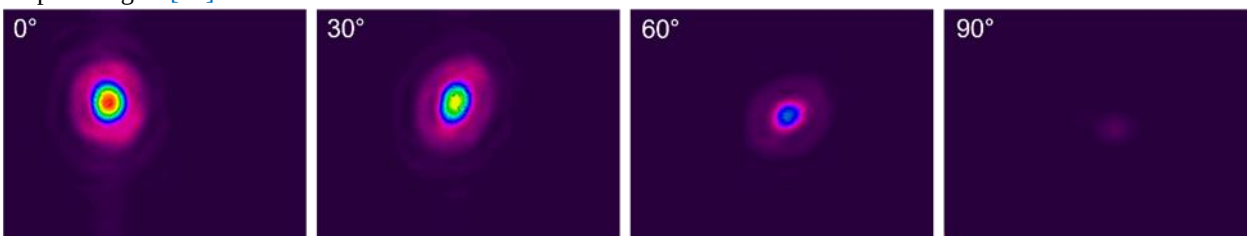

Fig. 5. Transmitted Intensity and beam deviation when rotating POP polariser at λ = 1.064 μm. The deviation corresponds to angular offset of approximately 5 mR.

3.3 Transmission Losses

The source of the transmission loss at both 780 nm and 1064 nm aroused interest and was investigated. We first checked the plate mounting angles by measuring the deflection of the low intensity beams with POP polariser plates rotated to the vertical, (and top Cu plate removed) yielding an angle $\theta_{Bexp} = 67.7 \pm 0.1°$ hence ~ 0.7° below the ideal Brewster angle at 780 nm. (At 1.06 μm, the plate angles are within 0.3° of $\theta_B = 68.0°$). Recalculating the effect on the transmission of the P component at 780 nm, we obtain $T_p > 0.9995$/plate or $T_P = 0.998$ (0.2%) for 4 plates, almost neglible. Hence, the only remaining source of significant loss would appear to be either surface - or volume scatter, assuming residual birefringence is very low. Residual birefringence in CVD ZnSe has been measured to be < ±15 nm/cm at 633 nm [29] and this effect could introduce a slight rotation and ellipticity in transmitted polarisation. Assuming an average value of 10 nm/cm at 780 nm, and 0.43 cm thickness, this would give a wave shift of $(\Delta\lambda/\lambda) \sim 0.006$ or phase shift $\Delta\varphi_{max} = 2.0°$ between P and S components. The loss to the P component could then be $\sim (\cos 2°)^4 = 0.998$, hence very low.

Bryzgalov et al [30] measured the transmission properties of polycrystalline ZnSe in materials grown by CVD as well as CT (ceramics technology) and EV (evaporation deposition) where the materials differ in grain size and degree of crystal quality. The growth of crystalline grains is accompanied by self-purification and segregation of impurity atoms into the intercrystallite space, altering the RI of grain boundaries but measured to be small, $\Delta n \sim 10^{-3}$ so that refraction is neglible. Defects and grain boundaries created during crystal growth (randomly oriented) result in diffuse light scatter. CVD grown ZnSe had the smallest grain size, nearly perfect cubic crystal structure and the lowest attenuation coefficient, which at 1.1μm, yielded $\mu = 0.261$ cm^{-1}. If applied to the 4 plate POP polariser (L = 0.43 cm) near Brewster's angle, we obtain a transmission limited by scattering losses for the P polarised component, $T_P = \exp(-\mu L) = 0.89$, the correct order of magnitude. However, such a high attenuation coefficient is not consistent with observed ZnSe transmission curves (0.5 – 12mm thickness) [24] which are almost independent of plate thickness, except where absorption occurs in the MIR and visible spectrum – and if applied to a 12 mm thick sample at normal incidence, would yield a transmission (including reflection losses) $T \sim (0.816)^2 \times 0.73 = 0.49 << 0.70$ observed. Volume scatter therefore does not account for the loss in T_p.

The surface roughness of the polished plates was measured with a Wyko white light interferometer (NT 1100), yielding $R_a = 7.9 \pm 1.1$nm. Such a small residual roughness can still lead to optical scatter – but can be estimated from the total integrated scatter (TIS), given by the expression [31],

$$\mathrm{TIS} = R_0 \left[1 - exp - \left(\frac{4\pi R_q cos\theta_i}{\lambda}\right)^2\right] \qquad (4)$$

where R_0 is the surface reflectivity, R_q (~1.4Ra) is the RMS surface roughness, θ_i is the angle of incidence and λ is the incident wavelength. As diffuse scatter scales linearly with surface reflectivity, the scatter due to P polarisation at 780 nm is near zero (TIS(P) $<10^{-6}$) while for S polarisation, $TIR(S) \sim 0.532 \times 3.52 \times 10^{-3} = 1.9 \times 10^{-3}$ or 0.19% per face hence 1.5 % for 4 plates. Surface scatter therefore does not appear to account for the observed losses.

However, observation of significant light scattering was confirmed with a hand-held NIR camera (Find-R-Scope, Optical Systems, Inc.). Fig. 6 shows detected bright scatter from the ZnSe plates (first plate removed) imaged through the NIR camera into a mobile phone. Incident linear polarisation was rotated to horizontal, ie P polarisation where surface scatter should be neglible, according to equation 4. The scatter (780 nm) appeared uniform in all directions (forward and backward), however, the camera is probably saturated. The plates were polished to a 60/40 scratch dig and although we expect low level surface scatter for this surface finish, the polishing procedure with this poly-crystalline material likely results in crystal lattice damage on all faces, causing an unexpectedly high level of scatter which originates in thin, damaged surface layers. This was confirmed by measuring the scattered power with a sensitive Si detector (Coherent LM-2) while altering scattering angle and rotating incident polarisation using the HWP. Scatter from S polarisation was significanty higher than P polarisation suggesting that this is primarily surface generated. With the 0.5cm^2 area detector placed at 10cm from the first plate and 10° from the specular direction with incident power $P_i = 32$mW in P polarisation, the scattered power $P_s = 2.5$μW, falling off with increasing scatter angle approximately as $P_s \sim P_i \cos\theta$. If we now assume azimuthal independence and integrating power distribution over 4π steradian, (detector solid angle $\Omega = 5 \times 10^{-3}$ steradian) we obtain estimated integrated scatter $P_T \sim$ 3.3mW or 10%.

This is an overestimate as scatter from the second plate was also detected hence we find ~ 5% loss/plate in approximate agreement with observed losses. In a further demonstration, a 15 mm thick ZnSe lens (f = 150 mm) polished on all faces was exposed to the 780 nm laser beam. Bright scatter was observed only from the lens faces and no signal detected from the bulk material when viewing the lens side on through the wide, polished edge with the NIR camera.

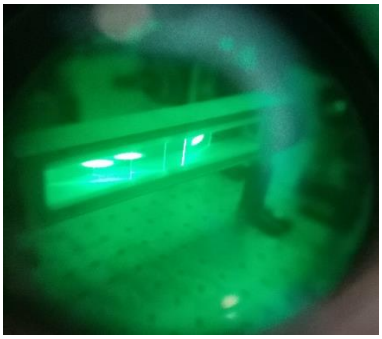

Fig. 6. Image captured through a hand held NIR camera with incident P polarisation at λ = 780 nm, showing bright scatter from plates (first plate removed). Although surface scatter should be low, this significant scatter likely originates in thin surface layers damaged by the polishing process.

With 3 × 1 mm thick plates and 3 × 4 mm polished plates available and tilted to Brewster's angle, the transmission was measured to be $T_p = 0.723 \pm 0.006$ with $T_s = 0.0012 \pm 5.6.\ 10^{-6}$ hence an extinction ratio of 1.66×10^{-3} or 1/600. The P polarisation losses with 6 plates corresponds to the observed linear reduction with plate number, not plate thickness.

Finally, one might also consider whether non-linear absorption could contribute to the unexpected optical losses, however, recent work on 2-photon absorption in polycrystalline ZnSe at 775 nm with femtosecond laser pulses measured the 2-photon absorption coefficient $\beta = 3.5$ cmGW^{-1} at peak intensities I < 5 GW cm^{-2} [32]. As incident peak intensities here with 10ns pulses $I_0 = 5 \times 10^4$Wcm^{-2}, then transmission loss due to NL absorption in 4 plates and P polarisation $T \sim (1+\beta I_0 z)^{-1} = 0.99992$, thus neglible. At λ = 1.06 μm, with photon energy hν =1.07 eV and material bandgap of 2.7 eV [30], it would require 3-photon absorption to induce losses, even less probable.

The likely performance of the POP polariser at longer wavelengths in the NIR and MIR can be inferred from the tabulated variation in the refractive index [24]. Fig. 7 shows the calculated Brewster angle from the visible range to the NIR and MIR in ZnSe where dispersion becomes very low. The Brewster angle in ZnSe varies by < 1° over the range 1-18 μm hence the POP performance should be equivalent or superior to that measured at 1.06 μm since absorption becomes insignificant (α < 0.001 cm^{-1}) combined with a potentially lower level of scattering as wavelength increases.

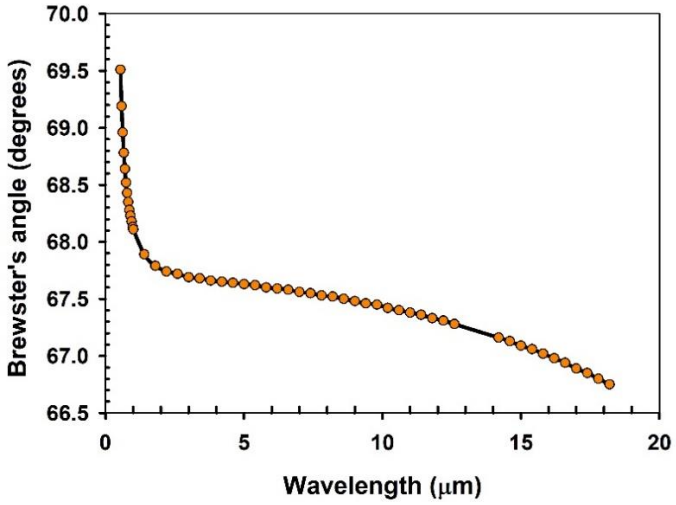

Fig. 7. Brewster's angle versus wavelength for ZnSe calculated from the variation in refractive index [24]. The Brewster angle varies by < 1° over the range 1 - 18 μm hence POP polariser would have a large bandwidth.

4 Conclusions

A POP polariser based on polycrystalline ZnSe was constructed with plates having rectangular dimensions of 28 × 50 × 1.0 mm. The DOP was measured in the NIR at 780 nm for 1 - 4 plates and compared with theoretical calculation based on the Airy expressions, yielding excellent agreement while the observed extinction ratio $E < 10^{-2}$ with $DOP_{exp} = 0.98$. The polariser also performed well at 1.06 μm with a similar extinction ratio and angular offset < 5 mR. With 6 plates (3 × 1 mm thick plates plus 3 × 4 mm thick plates) tilted to Brewster's angle, the transmission was measured to be $T_p = 0.723 \pm 0.006$ with $T_s = 0.0012 \pm 5.6 \times 10^{-6}$, achieving an extinction ratio of 1.66×10^{-3} or 1/600. It was observed that the absolute transmission of incident P-polarisation T_p at both wavelengths was lower than expected from the given absorption coefficients, measured residual specular reflection, estimated surface scatter, volume scatter and residual birefringence. These effects were calculated and could not account for the level of measured transmission losses. However, from our observations of scatter using a hand-held NIR camera, this drop in absolute transmission, we believe is primarily due to residual surface scatter from thin damaged crystal lattice surface regions, created during the polishing process of polycrystalline ZnSe. This was confirmed by measuring the approximate angular scattered power distribution and when integrated over 4π solid angle, corresponds to about 5% per plate in approximate agreement with observed losses. T_p scales almost linearly with plate number, not plate thickness. Clearly, more careful angular scatter measurements could be undertaken in the future as well as a study of the performance of plates polished to a much better surface finish. As dispersion (and absorption) is very low between 1-16 μm in the MIR, this type of polariser should have similar characteristics over this important spectral region although scatter may well reduce with wavelength. The device would also be a useful polariser for low power ($P \leq 10W$) randomly polarised CO_2 laser beams or as polarisation analyser for NIR and MIR spectral sources.

CRediT authorship contribution statement

Qianliang Li conducted the experiments and wrote the paper. Walter Perrie conceived the work, directed the experiments and co-wrote paper. Tong Zhou and Zheng Fang performed the transmission measurements at 1.064 μm. Stuart Edwardson and Geoff Dearden directed and supervised the research. All authors discussed the results and commented on the manuscript.

Declaration of competing interest

The authors declare that they have no known competing financial interests or personal relationships that could have appeared to influence the work reported in this paper.

Acknowledgements

We would like to thank Mr. Andy Snaylam, technician in the Laser Group, UOL who fabricated the Pile-of-Plates polariser assembly. We also thank Keith Matthews of Crystran Ltd, UK for technical support on optical properties of ZnSe.

References

[1] E. Komatsu, New physics from the polarised light of the cosmic microwave background, arXiv e-prints arXiv:2202.13919 (2022).

[2] H. Kleinpoppen, Electron Photon Coincidences and Polarization of Impact Radiation, in Fourth International Conference on Atomic Physics (eds. Putilitz, G., Weber, E. & Winnaker, A.) (Plenum Press, NY and London), Heidelberg. (1975).

[3] G., K., T., G. Conn, K., Eaton, On the Analysis of Elliptically Polarized Radiation in the Infrared Region, J. Opt. Soc. Am. 44 (1954) 546–551.

[4] C. Rosales-Guzmán, B. Ndagano, A. Forbes, A review of complex vector light fields and their applications, J. Opt. 20 (2018) 123001-.

[5] Y. Intaravanne, X. Chen, Recent advances in optical metasurfaces for polarization detection and engineered polarization profiles, 9 (2020) 1003–1014. https://doi.org/doi:10.1515/nanoph-2019-0479.

[6] M. Bennet, Handbook of optics., Vol.2. 2nd ed., Ch.3, ed M Bass. McGraw-Hill, (1995)..

[7] Calcite Optical Material, (n.d.). https://www.crystran.co.uk/optical-materials/calcite-caco3 (accessed May 4, 2022).

[8] A.. Fresnel, Oevres Complete, 10 (1866) 640–648.
[9] G.G. Stokes, IV. On the intensity of the light reflected from or transmitted through a pile of plates, Proc. R. Soc. London. 11 (1862) 545–556. https://doi.org/10.1098/rspl.1860.0119.
[10] L.B. Tuckerman, On the Intensity of the Light Reflected from or Transmitted through a Pile of Plates, J. Opt. Soc. Am. 37 (1947) 818–825. https://doi.org/10.1364/JOSA.37.000818.
[11] G.K.T. Conn, G.K. Eaton, On Polarization by Transmission with Particular Reference to Selenium Films in the Infrared, J. Opt. Soc. Am. 44 (1954) 553. https://doi.org/10.1364/JOSA.44.000553.
[12] R.G. Greenler, K.W. Adolph, G.H. Emmons, A compact polarizer for the infrared, Appl. Opt. 5 (1966) 1468–1469.
[13] J.L. Weinberg, On the Use of a Pile-of-Plates Polarizer---The Transmitted Component, Appl. Opt. 3 (1964) 1057–1061. https://doi.org/10.1364/AO.3.001057.
[14] W. Perrie, A.J. Duncan, H.J. Beyer, H. Kleinpoppen, Polarization Correlation of the Two Photons Emitted by Metastable Atomic Deuterium: A Test of Bell's Inequality, Phys. Rev. Lett. 54 (1985) 1790–1793. https://doi.org/10.1103/PhysRevLett.54.1790.
[15] J.S. Bell, On the Problem of Hidden Variables in Quantum Mechanics, Rev. Mod. Phys. 38 (1966) 447–452. https://doi.org/10.1103/RevModPhys.38.447.
[16] A. Aspect, Experimental Tests of Bell's Inequalities BT - The Wave-Particle Dualism: A Tribute to Louis de Broglie on his 90th Birthday, in: S. Diner, D. Fargue, G. Lochak, F. Selleri (Eds.), Springer Netherlands, Dordrecht, 1984: pp. 377–390. https://doi.org/10.1007/978-94-009-6286-6_20.
[17] S.-E. Kim, J.-R. Park*, Analysis of an Ultraviolet Polarizer by Using a Pile of Fused Quartz Plates, Orig. New Phys. Sae Mulli. 70 (2020) 692–697. https://doi.org/10.3938/NPSM.70.692.
[18] M. Piwiński, D. Dziczek, Ł. Kłosowski, S. Chwirot, Experimental investigation of electron impact excitation of zinc atoms to the 41P1 state, Eur. Phys. J. Spec. Top. 222 (2013) 2273–2277. https://doi.org/10.1140/epjst/e2013-02005-0.
[19] M. Lintz, J. Guéna, M.-A. Bouchiat, D. Chauvat, Demonstration of an optical polarization magnifier with low birefringence, Rev. Sci. Instrum. 76 (2005) 43102. https://doi.org/10.1063/1.1879292.
[20] H.N. Rutt, A low-cost, ultra-wide-range infrared polarizer, Meas. Sci. Technol. 6 (1995) 1124.
[21] D.J. Dummer, S.G. Kaplan, L.M. Hanssen, A.S. Pine, Y. Zong, High-Quality Brewster's Angle Polarizer for Broadband Infrared Application., Appl. Opt. 37 (1998) 1194–1204. https://doi.org/10.1364/ao.37.001194.
[22] B. Csanaková, O. Novák, M. Smrž, J. Huynh, H. Jelínková, A. Lucianetti, T. Mocek, Silicon Brewster plate wavelength separator for a mid-IR optical parametric source., Appl. Opt. 60 (2021) 281–290. https://doi.org/10.1364/AO.411408.
[23] Q. Zhang, H. Li, Y. Ma, T. Zhai, ZnSe nanostructures: Synthesis, properties and applications, Prog. Mater. Sci. 83 (2016) 472–535. https://doi.org/https://doi.org/10.1016/j.pmatsci.2016.07.005.
[24] Zinc Selenide (ZnSe) Optical Material, (n.d.). https://www.crystran.co.uk/optical-materials/zinc-selenide-znse (accessed July 21, 2021).
[25] T.A. Leonard, J. Loomis, K.G. Hardina, M. Scott, Design And Construction Of Three Infrared Ellipsometers For Thin Film Research, Opt. Eng. 21 (1982) 971. https://doi.org/10.1117/12.7973016.
[26] G.R. Fowles, Introduction to modern optics, 2nd ed., Dover Publications, 1975.
[27] H. Qi, X. Zhang, M. Jiang, Q. Wang, D. Li, Optical Constants of Zinc Selenide in Visible and Infrared Spectral Ranges, J. Appl. Spectrosc. 84 (2017) 679–682. https://doi.org/10.1007/s10812-017-0529-9.
[28] G.R. Bird, W.A. Shurcliff, Pile-of-plates polarizers for the infrared: improvement in analysis and design, JOSA. 49 (1959) 235–237.
[29] S.P. Rummel, H.E. Reedy, G.L. Herrit, Residual stress birefringence in ZnSe and multispectral ZnS, in: Proc.SPIE, 1994. https://doi.org/10.1117/12.187335.
[30] A.N. Bryzgalov, V. V Musatov, V. V Buz'ko, Optical properties of polycrystalline zinc selenide, Semiconductors. 38 (2004) 310–312. https://doi.org/10.1134/1.1682334.
[31] H.E. Bennett, J.O. Porteus, Relation Between Surface Roughness and Specular Reflectance at Normal Incidence, J. Opt. Soc. Am. 51 (1961) 123–129. https://doi.org/10.1364/JOSA.51.000123.
[32] Q. Li, W. Perrie, Z. Li, S.P. Edwardson, G. Dearden, Two-photon absorption and stimulated emission in poly-crystalline Zinc Selenide with femtosecond laser excitation, Opto-Electronic Adv. 5 (2022) 210012–210036. https://doi.org/10.29026/oea.2022.210036.